

## Octakis(dimethylammonium) hexa- $\mu_2$ -chlorido-hexachloridotrinickelate(II) dichloride: a linear trinickel complex with asymmetric bridging

Allison Gerdes and Marcus R. Bond\*

Department of Chemistry, Southeast Missouri State University, Cape Girardeau, MO 63701, USA

Correspondence e-mail: bond@mbond2.st.semo.edu

Received 3 September 2009

Accepted 11 September 2009

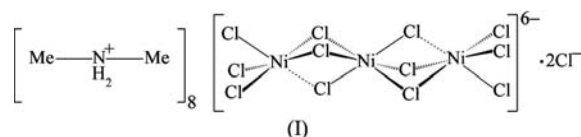
Online 26 September 2009

The title compound,  $(C_2H_8N)_8[Ni_3Cl_{12}]Cl_2$ , crystallizes as linear  $[Ni_3Cl_{12}]^{6-}$  complex anions with inversion symmetry, separated from one another by dimethylammonium cations and noncoordinated chloride ions. The gross structural arrangement of the trinickel complex is as a segment of face-sharing  $NiCl_6$  octahedra similar to the  $(NiCl_3)_n$  chains of  $CsNiCl_3$ -type compounds. On closer inspection, the regular coordination geometry of the complex consists of octahedral  $NiCl_6$  in the center linked by two symmetrically bridging chloride ions to square-pyramidal  $NiCl_5$  on each end. A long semicoordinate bond is formed by each of the terminal  $Ni^{II}$  cations, to give a 5+1 coordination geometry and form an asymmetric bridge to the central  $Ni^{II}$  cation. The dimethylammonium cations surround the complex with an extensive hydrogen-bonding network, linking the complex to the noncoordinated chloride ions. Asymmetric bridging in the complex arises from short hydrogen bonds from the same dimethylammonium cation to the apical and asymmetric bridging chloride ions, causing the complex to scissor outward.

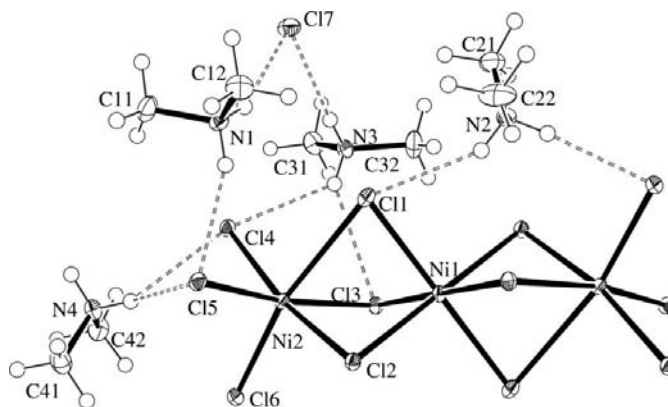
### Comment

The  $CsNiCl_3$  structure type, consisting of parallel chains of face-sharing  $NiCl_6$  octahedra, is a dominant motif of nickel(II) chloride structural chemistry.  $ANiCl_3$  compounds of this type are readily formed with a variety of organic cations, and are found to exhibit only minor distortions from regular octahedral coordination and to contain tri- $\mu_2$ -symmetric chloride bridges between neighbors (Bond, 1990). This structure type is even found for a different stoichiometric combination of  $ACl$  and  $NiCl_2$ , specifically for  $(piperidinium)_2NiCl_4$ , which consists of parallel  $(NiCl_3)_n$  chains and noncoordinated chloride ions rather than the isolated tetrahedral or square-planar  $[NiCl_4]^{2-}$  complexes one might first expect (Bond & Willett, 1993). This predictable structural regularity is in marked contrast to copper(II) chloride compounds, the structures and composi-

tions of which are extremely dependent on the structure of the organic counter-ion (Willett, 1991). Copper(II) chloride chain structures are frequently found with a mixture of symmetric and asymmetric chloride bridges, the latter a result of long semicoordinate bonding produced by the Jahn–Teller-distorted  $Cu^{II}$  coordination polyhedra. The title compound, (I), contains a linear trinickel complex which appears similar to a chain segment from an  $ANiCl_3$  compound, but with some intriguing differences which suggest that a more complicated structural chemistry for nickel(II) chlorides remains to be explored.



The linear trinickel complex of (I) consists of an octahedral  $NiCl_6$  group ( $Ni1$ ) located at the center of the complex, and also on an inversion center, and two terminal  $NiCl_5$  groups. The central  $Ni^{II}$  cation exhibits minor distortions from octahedral coordination: the  $Ni1-Cl$  bond lengths are in the range  $\sim 2.40-2.45$  Å, with the  $Ni1-Cl1$  bond the longest, and the  $Cl-Ni1-Cl$  angles deviate by only  $4-5^\circ$  from right angles (Table 1). The interior  $Cl-Ni1-Cl$  angles are acute, a consequence of elongation of the octahedron along its trigonal axis, which results from electrostatic repulsion between neighboring metal cations. The coordinate bonds of the terminal nickel ions form a square-pyramidal arrangement, with atom  $Cl6$  as the apical ligand. The  $Ni2-Cl$  coordinate bond lengths fall in the narrow range  $\sim 2.36-2.38$  Å, except for  $Ni-Cl3$  which is  $\sim 0.10$  Å longer. Deviations in the  $Ni-Cl$  coordinate bond of this magnitude resulting from crystal packing strains have been observed previously for the  $[NiCl_6]^{4-}$  complex in  $(3\text{-chloroanilinium})_8NiCl_{10}$  (Wei &


**Figure 1**

The  $[Ni_3Cl_{12}]^{6-}$  complex anion of (I), surrounded by the chloride anion and dimethylammonium cations of the asymmetric unit, showing the atom-numbering scheme. Displacement ellipsoids are drawn at the 50% probability level and H atoms are shown as small spheres of arbitrary radii. Significant hydrogen-bonding interactions are shown as dashed lines.

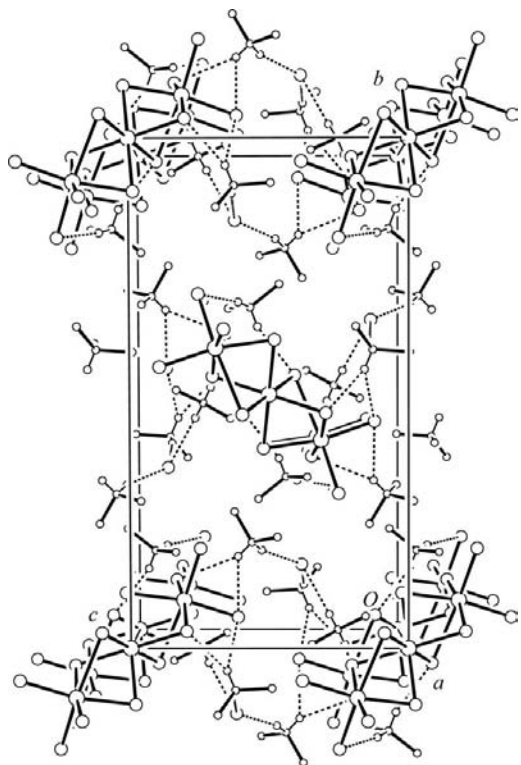


**Figure 2**

A packing diagram for (I), viewed along the *a* axis. Hydrogen bonding that establishes the layered packing arrangement of the trinickel complexes is shown as dashed lines.

Willett, 1995). Atom Ni2 is 0.2172 (2) Å above the basal plane and completes its coordination environment by forming a long semicoordinate bond (0.3–0.4 Å longer than the coordinate bonds) to atom Cl1, to give it a 5+1 coordination geometry, while also forming an asymmetric bridge to atom Ni1. The bond lengths and angles within the dimethylammonium cations conform to expected values (Ladd & Palmer, 1994). Fig. 1 shows the complex anion grouped with other ions of the asymmetric unit. Bond lengths and angles of the complex anion are presented in Table 1.

The extended structure of (I) can be envisioned as square-packed layers of trinickel complexes parallel to the *ac* plane and stacked along the *b* axis, with all complexes within a layer translationally equivalent. The axis of the complex centered at the origin of the unit cell (as determined by the Ni1–Ni2 vector) points approximately along the  $[2\bar{1}2]$  line and forms angles of 59.60 (1), 44.49 (1) and 49.43 (1)° with the *a*, *b* and *c* axes, respectively. Neighboring layers are related by a *c*-glide operation, which reverses the orientation of the complex and places the complexes at inversion centers on the corners and in the centers of the *bc* faces of the unit cell. Complex ions, dimethylammonium cations and noncoordinated chloride ions can be envisioned as forming parallel lines of translationally equivalent ions along the *a* axis. A packing diagram viewed down the *a* axis is shown in Fig. 2.

Each complex is surrounded by a cage of eight dimethylammonium cations. Cation 1 (N1) is found deepest within the

square-packed layers of complexes and forms hydrogen bonds to atom Cl5 in the complex and to the noncoordinated Cl7 chloride ion. Cation 2 (N2) forms hydrogen bonds to chloride ions Cl1 and Cl6 in the same complex, while cation 3 (N3) forms a hydrogen bond to atom Cl7 and a bifurcated hydrogen bond to atoms Cl3 and Cl4. Cation 4 (N4) is the one most exterior to the layer, and forms a bifurcated hydrogen bond to two terminal chloride ions and one hydrogen bond to atom Cl7. The hydrogen bonds involving the chloride ions in the complex and the noncoordinated chloride ions form a network that indirectly links the complexes into a chain parallel to  $[110]$  in the same layer. Significant hydrogen-bonding interactions are summarized in Table 2.

Noncoordinated chloride ions are sequestered close to the  $x = \frac{1}{2}$  plane in the unit cell and between the complexes. This packing arrangement is similar to the sequestration of noncoordinated iodide ions in  $[\text{Co}(\text{en})_3]_4(\text{Sn}_3\text{I}_{12})\text{I}_2$  (en is ethylenediamine; Lode & Krautscheid, 2007), the only other  $[\text{M}_3\text{X}_{12}]^{n-}$  compound with noncoordinated halides. However, in the iodide compound, the  $[\text{Co}(\text{en})_3]^{2+}$  ions form more clearly defined channels in which the noncoordinated iodide anions can reside.

The complex in (I) bears a strong resemblance to the structure of the complex in (dimethylammonium) $_6\text{Cr}_3\text{Cl}_{12}$  [Babar *et al.*, 1981; refcode BAHVOV in the Cambridge Structural Database (Allen, 2002)]. The trichromium complex can also be considered to have two symmetric bridges and one asymmetric bridge from the central to each terminal metal atom. Here, the distortions of the bridging and coordination geometries were attributed to the strong Jahn–Teller activity expected for  $\text{Cr}^{\text{II}}$ . The coordination geometries of  $\text{Ni}^{\text{II}}$  in (I) do show less distortion than found for  $\text{Cr}^{\text{II}}$  in  $[\text{Cr}_3\text{Cl}_{12}]^{6-}$ , almost certainly a consequence of the absence of Jahn–Teller activity expected for  $\text{Ni}^{\text{II}}$ . But why does  $[\text{Ni}_3\text{Cl}_{12}]^{6-}$  show any distortion at all? In this case it appears that the complex distorts so as to better accommodate the hydrogen bonding established by the organic cation ‘cage’ that surrounds it. It is notable that the shortest and most direct hydrogen bond made to the complex is to the apical chloride ion of one terminal  $\text{Ni}^{\text{II}}$  ion  $[\text{H}2\text{A} \cdots \text{Cl}6(-x, -y, -z)]$ . This same cation also forms a short hydrogen bond to the asymmetrically bridged chloride ion of the other terminal  $\text{Ni}^{\text{II}}$  ion  $(\text{H}2\text{B} \cdots \text{Cl}1)$ . In this way, the hydrogen bonding from cation 2 induces a scissoring action on the complex that opens it up and establishes the asymmetric bridge. A similar hydrogen-bonding arrangement is present in BAHVOV, with  $\text{N} \cdots \text{Cl}$  distances to the apical and asymmetric bridge chloride ions (3.163 and 3.210 Å, respectively) that are comparable to those in (I). Thus, while much of the distortion in the  $[\text{Cr}_3\text{Cl}_{12}]^{6-}$  complex can be attributed to the Jahn–Teller effect, a significant contribution to the distortion of the bridging geometry is probably induced by hydrogen bonding. Dramatic distortions in bridging geometry caused by hydrogen bonding are known. For example, the V–O–V bridging angle in  $\mu_2$ -oxido-bis[bis(L-histidine)vanadium(III)] is reduced by almost 30° as a result of hydrogen bonding between histidine ligands on neighboring  $\text{V}^{\text{III}}$  cations (Czerszewicz *et al.*, 1994).

Experimental

Crystals of (I) were grown by slow evaporation of an approximately 6 M HCl solution containing dimethylammonium chloride and nickel(II) chloride dissolved in a 3:1 molar ratio. The solution was maintained at a temperature of 323 K. While small crystals of (I) were orange in color under the microscope, the bulk sample was dark burgundy red.

Crystal data

(C<sub>2</sub>H<sub>8</sub>N)<sub>8</sub>[Ni<sub>3</sub>Cl<sub>12</sub>]Cl<sub>2</sub>  
*M<sub>r</sub>* = 1041.18  
 Monoclinic, *P*2<sub>1</sub>/*c*  
*a* = 10.0058 (2) Å  
*b* = 20.0564 (4) Å  
*c* = 10.9787 (2) Å  
 β = 92.464 (1)°  
*V* = 2201.17 (7) Å<sup>3</sup>  
*Z* = 2  
 Mo *K*α radiation  
 μ = 2.14 mm<sup>-1</sup>  
*T* = 100 K  
 0.27 × 0.24 × 0.21 mm

Data collection

Bruker KappaCCD diffractometer  
 Absorption correction: multi-scan  
 (DENZO/SCALEPACK;  
 Otwinowski & Minor, 1997)  
*T<sub>min</sub>* = 0.564, *T<sub>max</sub>* = 0.635  
 34160 measured reflections  
 18194 independent reflections  
 13786 reflections with *I* > 2σ(*I*)  
*R<sub>int</sub>* = 0.031

Refinement

*R*[*F*<sup>2</sup> > 2σ(*F*<sup>2</sup>)] = 0.032  
*wR*(*F*<sup>2</sup>) = 0.052  
*S* = 1.08  
 18194 reflections  
 228 parameters  
 H atoms treated by a mixture of independent and constrained refinement  
 Δρ<sub>max</sub> = 0.57 e Å<sup>-3</sup>  
 Δρ<sub>min</sub> = -0.76 e Å<sup>-3</sup>

Table 1

Selected geometric parameters (Å, °).

Ni1—Cl1	2.44795 (18)	Ni2—Cl3	2.47116 (19)
Ni1—Cl2	2.40560 (17)	Ni2—Cl4	2.3612 (2)
Ni1—Cl3	2.40999 (17)	Ni2—Cl5	2.3718 (2)
Ni2—Cl1	2.8168 (2)	Ni2—Cl6	2.3832 (2)
Ni2—Cl2	2.3742 (2)		
Cl1—Ni1—Cl2	86.056 (6)	Cl2—Ni2—Cl6	94.197 (7)
Cl1—Ni1—Cl3	85.088 (6)	Cl3—Ni2—Cl4	92.661 (7)
Cl2—Ni1—Cl3	86.020 (6)	Cl3—Ni2—Cl5	169.726 (8)
Cl2—Ni2—Cl3	85.341 (6)	Cl3—Ni2—Cl6	92.842 (7)
Cl1—Ni2—Cl2	78.784 (6)	Cl4—Ni2—Cl5	88.287 (7)
Cl1—Ni2—Cl3	76.496 (6)	Cl4—Ni2—Cl6	96.485 (7)
Cl1—Ni2—Cl4	90.445 (7)	Cl5—Ni2—Cl6	97.218 (7)
Cl1—Ni2—Cl5	93.271 (7)	Ni1—Cl1—Ni2	74.277 (5)
Cl1—Ni2—Cl6	167.577 (7)	Ni1—Cl2—Ni2	83.798 (6)
Cl2—Ni2—Cl4	169.218 (8)	Ni1—Cl3—Ni2	81.672 (6)
Cl2—Ni2—Cl5	91.823 (7)		

All H atoms were visible in difference maps. The positions of the methyl group H atoms were calculated and constrained during refinement using a riding model [C—H = 0.96 Å and *U*<sub>iso</sub>(H) = 1.5*U*<sub>iso</sub>(C)]. The positions and isotropic displacement parameters of H atoms bound to N atoms were freely refined. The refined N—H bond lengths are in the range 0.837 (14)–0.868 (14) Å and the displacement parameters are in the range 0.021 (3)–0.030 (4) Å<sup>2</sup>.

Table 2

Hydrogen-bond geometry (Å, °).

<i>D</i> —H... <i>A</i>	<i>D</i> —H	H... <i>A</i>	<i>D</i> ... <i>A</i>	<i>D</i> —H... <i>A</i>
N1—H1A...Cl7	0.868 (14)	2.407 (14)	3.2222 (8)	156.5 (12)
N1—H1B...Cl5	0.862 (13)	2.380 (14)	3.1901 (8)	156.8 (11)
N2—H2A...Cl6 <sup>i</sup>	0.868 (13)	2.311 (13)	3.1696 (8)	170.2 (12)
N2—H2B...Cl1	0.837 (14)	2.501 (14)	3.2525 (8)	149.9 (12)
N3—H3A...Cl7	0.865 (13)	2.289 (14)	3.1409 (7)	168.2 (12)
N3—H3B...Cl3	0.855 (15)	2.752 (15)	3.4812 (8)	144.2 (12)
N3—H3B...Cl4	0.855 (15)	2.507 (14)	3.1448 (7)	132.1 (12)
N4—H4A...Cl7 <sup>ii</sup>	0.857 (14)	2.351 (14)	3.1786 (8)	162.6 (12)
N4—H4B...Cl4	0.840 (14)	2.600 (14)	3.2705 (7)	137.7 (12)
N4—H4B...Cl5	0.840 (14)	2.746 (14)	3.4360 (8)	140.5 (11)

Symmetry codes: (i) -*x*, -*y*, -*z*; (ii) -*x* + 1, -*y*, -*z* + 1.

Data collection: COLLECT (Nonius, 1998); cell refinement: SCALEPACK (Otwinowski & Minor, 1997); data reduction: DENZO (Otwinowski & Minor, 1997) and SCALEPACK; program(s) used to solve structure: SIR92 (Altomare *et al.*, 1994); program(s) used to refine structure: SHELXL97 (Sheldrick, 2008); molecular graphics: ORTEP-3 for Windows (Farrugia, 1997) and ORTEP-III (Burnett & Johnson, 1996); software used to prepare material for publication: WinGX (Farrugia, 1999).

The authors thank the National Science Foundation DUE CCLI-A&I program (grant No. 9951348) and Southeast Missouri State University for funding the X-ray diffraction facility.

Supplementary data for this paper are available from the IUCr electronic archives (Reference: DN3125). Services for accessing these data are described at the back of the journal.

References

Allen, F. H. (2002). *Acta Cryst.* **B58**, 380–388.  
 Altomare, A., Casciarano, G., Giacovazzo, C., Guagliardi, A., Burla, M. C., Polidori, G. & Camalli, M. (1994). *J. Appl. Cryst.* **27**, 435.  
 Babar, M. A., Ladd, M. F. C., Larkworthy, L. F., Povey, D. C., Proctor, K. J. & Summers, L. J. (1981). *J. Chem. Soc. Chem. Commun.* pp. 1046–1047.  
 Bond, M. R. (1990). PhD thesis, Washington State University, USA.  
 Bond, M. R. & Willett, R. D. (1993). *Acta Cryst.* **C49**, 668–671.  
 Burnett, M. N. & Johnson, C. K. (1996). *ORTEP-III*. Report ORNL-6895. Oak Ridge National Laboratory, Tennessee, USA.  
 Czernuszewicz, R. S., Yan, Q., Bond, M. R. & Carrano, C. J. (1994). *Inorg. Chem.* **33**, 6116–6119.  
 Farrugia, L. J. (1997). *J. Appl. Cryst.* **30**, 565.  
 Farrugia, L. J. (1999). *J. Appl. Cryst.* **32**, 837–838.  
 Ladd, M. F. C. & Palmer, R. A. (1994). *Structure Determination by X-ray Crystallography*, 3rd ed., pp. 434–435. New York: Plenum Press.  
 Lode, C. & Krautscheid, H. (2007). *Z. Anorg. Allg. Chem.* **633**, 1691–1694.  
 Nonius (1998). *COLLECT*. Nonius BV, Delft, The Netherlands.  
 Otwinowski, Z. & Minor, W. (1997). *Methods in Enzymology*, Vol. 276, *Macromolecular Crystallography*, Part A, edited by C. W. Carter Jr & R. M. Sweet, pp. 307–326. New York: Academic Press.  
 Sheldrick, G. M. (2008). *Acta Cryst.* **A64**, 112–122.  
 Wei, M. & Willett, R. D. (1995). *Inorg. Chem.* **34**, 3780–3784.  
 Willett, R. D. (1991). *Coord. Chem. Rev.* **109**, 181–205.